

# The Radio Loud / Radio Quiet dichotomy: news from the 2dF QSO Redshift Survey

M. Cirasuolo, M. Magliocchetti, A. Celotti, L. Danese

*SISSA, Via Beirut 4, 34014, Trieste, Italy*

7 November 2018

## ABSTRACT

We present a detailed analysis of a sample of radio-detected quasars, obtained by matching together objects from the FIRST and 2dF Quasar Redshift Surveys. The dataset consists of 113 sources, spanning a redshift range  $0.3 \lesssim z \lesssim 2.2$ , with optical magnitudes  $18.25 \leq b_J \leq 20.85$  and radio fluxes  $S_{1.4\text{GHz}} \geq 1$  mJy. These objects exhibit properties such as redshift and colour distribution in full agreement with those derived for the whole quasar population, suggestive of an independence of the mechanism(s) controlling the birth and life-time of quasars of their level of radio emission. The long debated question of radio-loud (RL)/radio-quiet (RQ) dichotomy is then investigated for the combined FIRST-2dF and FIRST-LBQS sample, since they present similar selection criteria. We find the fraction of radio detections to increase with magnitude from  $\lesssim 3\%$  at the faintest levels up to  $\sim 20\%$  for the brightest sources.

The classical RL/RQ dichotomy, in which the distribution of radio-to-optical ratios and/or radio luminosities shows a lack of sources, is ruled out by our analysis. We also find no tight relationship between optical and radio luminosities for sources in the considered sample, result that tends to exclude the mass of the quasar black hole as the physical quantity associated to the level of radio emission.

**Key words:** galaxies: active - cosmology: observations - radio continuum: quasars

## 1 INTRODUCTION

It was soon realized that not all the quasars, though first discovered by Schmidt in 1963 at radio wavelengths, are powerful radio sources (Sandage 1965). Several optically selected quasar samples have been observed in radio (e.g. Sramek & Weedman 1980; Condon et al. 1981; Marshall 1987; Miller, Peacock & Mead 1990; Kellermann et al. 1989), showing that typically only 10% - 40% of the quasars are radio detected.

From these studies it was suggested that quasars can be divided into the two different populations of “Radio-Loud” and “Radio-Quiet” on the basis of their radio emission. Kellermann et al. (1989), performing VLA observations of the Palomar-Green Bright Quasar Survey (the so-called PG sample), found that the radio-to-optical ratios of these objects – defined as the ratio between radio and optical luminosity – presented a bimodal distribution, clearly showing the occurrence of these two different populations.

Miller, Peacock & Mead (1990) also found a dichotomy in the quasar population, although this time based on radio luminosity as the parameter to define the level of radio loudness.

A step forward in the study of the radio properties of quasars came with the FIRST Survey with the VLA (Becker, White & Helfand 1995) which was able to collect a large

sample of quasars at faint flux levels.

Recent works based on this survey (FIRST Bright Quasar Survey; White et al. 2000 and Large Bright Quasar Survey; Hewett et al. 2001) suggest that the RL/RQ dichotomy could be an effect due to the brighter radio and optical limits of the previous studies. The issue is however still under debate. A recent work by Ivezić et al. (2002), based on the cross-correlation of the Sloan Digital Sky Survey with the FIRST Survey seems to find clear evidence for bimodality (see also Goldschmidt et al. 1999).

From the theoretical point of view, despite the great advances in our ability of collecting unbiased sets of data, the physical mechanism(s) responsible for the radio emission in Active Galactic Nuclei is still unclear. It is generally accepted to be related to the processes of accretion onto a central black hole (BH) – the engine responsible for the optical-UV emission – but no correlation between radio and optical luminosity has been found so far in such objects (see e.g. Stocke et al. 1992). On the other hand, although controversial, there is some evidence for the fraction of radio-loud quasars to increase with increasing optical luminosity (Padovani 1993; La Franca et al. 1994; Hooper et al. 1995; Goldschmidt et al. 1999; but see also Ivezić et al. 2002 for a dissenting view), and more recent findings seem to identify the angular momentum of a spinning BH – extracted by a

arXiv:astro-ph/0301526v2 28 Jan 2003

magnetic field – as the correct mechanism to provide the necessary energy to fuel radio jets (for a review see Blandford 2000) and therefore turn a radio-quiet object into a radio-loud one.

A different approach deals with the possibility for radio loudness to be connected with the intrinsic properties of the host galaxy. Early studies in fact concluded that, while radio-loud quasars reside in elliptical hosts, radio-quiet ones are mainly found in spiral galaxies (Malkan 1984; Smith et al. 1986). Furthermore, it was observed a preference for radio-quiet quasars to be located in environments considerably less dense than those of radio-loud objects (Yee & Green 1987; Ellingson et al. 1991).

More recent studies (Dunlop et al. 2002; Finn et al. 2001) however find a very different picture whereby the hosts of both radio-loud and radio-quiet quasars are massive elliptical galaxies with basic properties (colors, environments, etc.) indistinguishable from those of quiescent, evolved, low-redshift ellipticals of comparable mass.

The aim of this work is then to analyze a wide sample of radio detected quasars drawn from the joined use of the FIRST and 2dF QSO Redshift Surveys in order to answer some of the questions raised throughout this section, with particular emphasis on the issue of radio-quiet/radio-loud dichotomy.

The layout of this paper is as follows. In Section 2 we give a brief description of the FIRST and 2dF datasets and of the matching procedure used to cross-correlate them, while in Section 3 we analyse the properties of the sample obtained from the joined use of these two surveys. In Section 4 we study the dependence on redshift and optical luminosity of the fraction of radio-detected quasars and in Section 5 we discuss the problem of radio loudness with particular attention devoted to the issue of radio-loud/radio-quiet dichotomy. In Section 6 we summarize our conclusions. Throughout this paper we will assume  $H_0 = 50 \text{ km s}^{-1} \text{ Mpc}^{-1}$ ,  $q_0 = 0.5$  and  $\Lambda = 0$ .

## 2 THE DATASETS

### 2.1 The FIRST Survey

The FIRST (Faint Images of the Radio Sky at Twenty centimeters) survey (Becker et al. 1995) began in 1993 and will eventually cover  $\sim 10,000$  square degrees of the sky in the North Galactic cap and equatorial zones. The beam-size at 1.4 GHz is 5.4 arcsec, with a rms sensitivity of typically 0.15 mJy/beam. Sources are detected using an elliptical Gaussian fitting procedure (White et al. 1997) with a  $5\sigma$  detection limit of  $\sim 1$  mJy. The positional accuracy in the FIRST survey is  $\lesssim 0.5$  arcsec at the 3 mJy level, reaching the value of 1 arcsec only at the survey threshold.

The latest release (5 July 2000) of the catalogue covers 7988 square degrees of the sky, including most of the area  $7^{\text{h}}20^{\text{m}} \lesssim \text{RA}(2000) \lesssim 17^{\text{h}}20^{\text{m}}$ ,  $22.2^\circ \lesssim \text{dec}(2000) \lesssim 57.5^\circ$  and  $21^{\text{h}}20^{\text{m}} \lesssim \text{RA}(2000) \lesssim 3^{\text{h}}20^{\text{m}}$ ,  $-2.8^\circ \lesssim \text{dec}(2000) \lesssim 2.2^\circ$ , and comprises approximately 722,354 sources down to a flux limit  $S_{1.4\text{GHz}} \simeq 0.8$  mJy. The surface density of objects in the catalogue is  $\sim 90$  per square degree, though this is reduced to  $\sim 80$  per square degree if one combines multi-component sources (Magliocchetti et al. 1998). The survey

has been estimated to be 95 per cent complete at 2 mJy and 80 per cent complete at 1 mJy (Becker et al. 1995). Note that, as the completeness level quickly drops for flux levels fainter than 1 mJy, in the following analysis we will only consider sources brighter than this limit.

### 2.2 The 2dF Quasar Redshift Survey

For the purposes of this work we have considered the first release of the 2dF QSO Redshift Survey, the so called *2QZ 10k catalogue*. A complete description of the catalogue can be found in Croom et al. (2001). Here we briefly recall its main properties. QSO candidates with  $18.25 \leq b_J \leq 20.85$  were selected from the APM catalogue (Irwin, McMahon & Maddox 1994) in two  $75^\circ \times 5^\circ$  declination strips centered on  $\delta = -30^\circ$  and  $\delta = 0^\circ$ , with colour selection criteria  $(u-b_j) \leq 0.36$ ;  $(u-b_j) < 0.12 - 0.8(b_j-r)$ ;  $(b_j-r) < 0.05$ . Such a selection guarantees a large photometric completeness ( $> 90\%$ ) for quasars within the redshift range  $0.3 \leq z \leq 2.2$ .

Redshifts for QSO candidates were determined via both cross-correlation of the spectra with specific templates (AUTOZ, Miller et al. in preparation) and by visual inspection. A flag was then assigned to each spectrum, where Q=1 corresponds to high quality identifications and redshift determinations, Q=2 means low-quality identifications and redshift determinations and Q=3 indicates no redshift assignment. Only 2dF fields with a spectroscopic completeness (defined as the ratio of objects observed in the field with Q=1 or Q=2 flags to the total number of spectroscopically observed objects) of 85 per cent or greater were included in this first release of the 2dF QSO catalogue. This corresponds to a mean overall completeness of 93 per cent which – by also allowing for sources not yet observed in the targeted fields – converts into an effective area for the survey of 289.6 square degrees (see Croom et al. 2001).

The final catalogue contains  $\sim 21,000$  objects with reliable (Q=1; Q=2) spectral and redshift determinations, out of which  $\sim 11,000$  are quasars ( $\sim 53\%$  of the sample). Whenever available, the 2QZ 10k catalogue also includes radio fluxes at 1.4 GHz from the NRAO VLA Sky Survey (NVSS; Condon et al. 1998) and X-ray fluxes from the ROSAT All Sky Survey (RASS; Voges et al. 1999).

### 2.3 Matching Procedure

The overlapping region between the FIRST and 2dF Quasar Redshift Surveys is confined to the equatorial plane:  $9^{\text{h}}50^{\text{m}} \leq \text{RA}(2000) \leq 14^{\text{h}}50^{\text{m}}$  and  $-2.8^\circ \leq \text{dec}(2000) \leq 2.2^\circ$ .

Optical counterparts for a subsample of FIRST radio sources have been obtained by matching together objects included in the radio catalogue with objects coming from the APM survey (Maddox et al. 1990) in the considered area (for a similar analysis see also McMahon et al. 2002). By following this procedure, Magliocchetti & Maddox (2002) find 4075 identifications – out of a total of  $\sim 24,000$   $S_{1.4\text{GHz}} \geq 1$  mJy radio sources – in the APM catalogue down to  $b_J \leq 22$  and for a matching radius of 2 arcsec. This last value was chosen after a careful analysis as the best compromise to maximize the number of real associations (estimated to be  $\sim 97\%$ ), and at the same time minimize the contribution from spurious identifications down to a negligible 5 per cent.

While this procedure has been proved to work for the population of radio sources as a whole since it mainly includes radio galaxies with point-like radio structures (Magliocchetti et al. 2002), caution needs to be taken when dealing with powerful radio sources such as quasars. These objects in fact often show multiple components such as jets and/or hot-spots.

The algorithm introduced by Magliocchetti et al. (1998) and adopted in this work to collapse sub-structured sources into single objects having radio fluxes equal to the sum of the fluxes of the various components, assigns positions to the final single-source products which correspond to the median point between the different sub-structures. Since multiple-component objects in general present quite complex morphologies, it can be possible that a number of “collapsed” sources end up with radio positions for their centroids which are displaced from their optical counterpart by more than the originally chosen value of 2 arcsec.

For this reason, we relax the requirement on the matching radius to 5 arcsec and consider as true optical identifications all the radio-optical pairs offset by less than this figure. Following the above procedure, we end up with 1044 identifications (hereafter called id-sample), down to a magnitude limit  $b_J = 20.85$ , which optically show point-like structures typical of the population of QSOs (see Magliocchetti & Maddox 2002 for further details).

Finally, in order to obtain redshift measurements and spectral features for these sources, we looked for objects in the 2QZ 10k catalogue with positions which differ by less than 2 arcsec from the optical positions of sources in the id-sample. The choice of this value for the matching radius is based on the 2 arcsec diameter of each 2dF fibre.

This procedure leads to 104 quasars included in the 2dF QSO catalogue and endowed with radio fluxes  $S_{1.4\text{GHz}} \geq 1$  mJy. The distribution of offsets between optical and radio positions is shown in Figure 1. Note that, despite the problems associated with multi-component structures discussed in this section, the overwhelming majority (> 90%) of identifications still lie within 2 arcsec from the corresponding radio position. As expected, only a few sources (almost all associated to multi-component structures) present offsets > 2".

As a final remark we note that, even though a choice for a larger matching radius in principle increases the number of spurious associations, this is not a concern in our analysis given the low space-density of 2dF quasars. In fact, for a 5 arcsec matching radius, the expected number of random coincidences on an area of 122 square degrees (effective area of the overlapping region between the FIRST and 2dF QSO Surveys) is about  $7 \times 10^{-2}$ .

### 2.4 FIRST vs NVSS

To double check the reliability of our sample and to also investigate the different efficiency of the FIRST and NVSS surveys in detecting sources, we have then compared objects from the sample obtained as in section 2.3 with those sources included in the 2QZ 10k catalogue and endowed with a radio-flux measurement from NVSS.

42 sources from the combined FIRST-2dF dataset do not present NVSS flux measurements in the 2QZ catalogue. A direct search for these objects in the NVSS on-

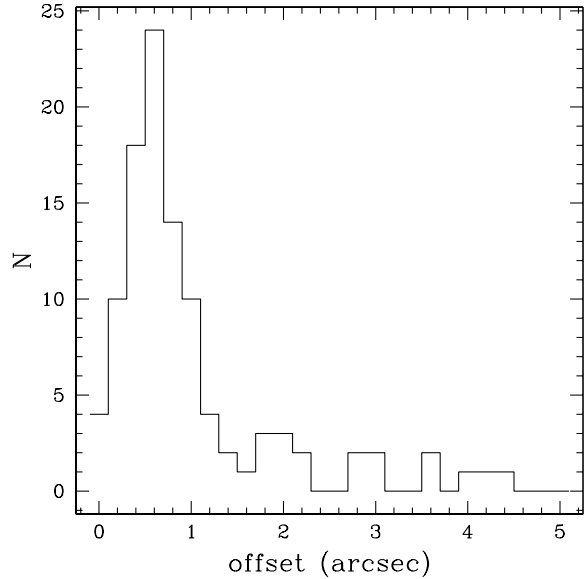


Figure 1. Distribution of offsets between radio and optical positions for the sub-sample of 2QZ 10k quasars included in the FIRST survey.

line database found 14 of them in the flux range  $3 \lesssim S_{1.4\text{GHz}} \lesssim 600$  mJy. Out of these 14 sources, three objects show multiple components and were therefore lost in the 2dF-NVSS matching procedure due to lack of a combining algorithm for sub-structured objects. Three more are instead single sources which show quite large radio-to-optical offsets (> 7 arcsec). The others are single objects with offsets  $\lesssim 3$  arcsec and it is not clear why they were not included in the 2QZ 10k catalogue.

The remaining 28 sources included in the combined FIRST-2dF catalogue show fluxes  $S_{1.4\text{GHz}} \lesssim 3$  mJy and were therefore lost by NVSS because of its relatively bright ( $\sim 3$  mJy; Condon et al. 1998) flux limit.

Following the same procedure as above, we also found 9 of the 2dF quasars with NVSS fluxes to be missed by our matching procedure. After a direct search, it turned out that six of them are double/triple sources, with positions for the centroids (as assigned by our combining procedure) which were displaced from the centers of the optical emission by more than 5 arcsec. The last three objects are instead point-like sources with radio-to-optical offsets between 5 and 7 arcsec and therefore lost by our searching criteria. These 9 sources have been added to our original FIRST-2QZ 10k dataset and appear in Table 1.

As a final remark, note that the high resolution of the FIRST survey (beaming size 5.4 arcsec) might imply some of the flux coming from extended sources to be resolved out, leading to a systematic underestimate of the real flux density of such sources. In order to check for this effect, we have compared FIRST and NVSS (which, having a lower resolution – beaming size of 45 arcsec – should not be affected by this problem) fluxes for all the sources in the 2QZ 10k catalogue which show a radio counterpart in both of these radio surveys. The result of the comparison is shown in Figure 2. It is clear that the agreement between fluxes as measured by

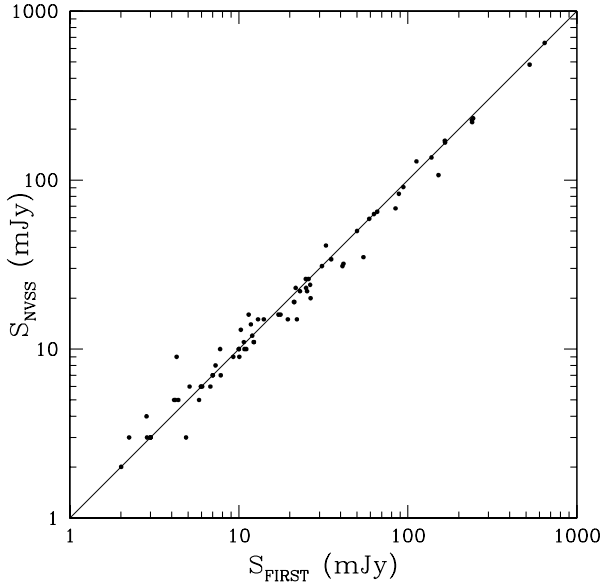


**Figure 2.** Comparison between 1.4 GHz fluxes as measured by the FIRST and NVSS Surveys for sources in the FIRST-2dF sample.

FIRST and NVSS is excellent and therefore no correction to the flux densities derived from the FIRST survey is needed.

### 3 THE SAMPLES

#### 3.1 FIRST-2dF

Based on the procedure described in the previous section, the sample derived from the joined use of the FIRST and 2dF QSO surveys is constituted by 113 objects (hereafter called the FIRST-2dF sample) with optical magnitudes  $18.25 \leq b_J \leq 20.85$  and radio fluxes at 1.4 GHz  $S_{1.4\text{GHz}} \geq 1$  mJy. All the objects included in the FIRST-2dF sample are presented in Table 1, whose columns respectively indicate:

- (1) 2dF name;
- (2) Right Ascension, RA(J2000) and Declination, dec(J2000) which – except for objects with multiple sub-structures where the coordinates indicate the centroid of the source (obtained as in Magliocchetti et al. 1998) – correspond to the FIRST radio coordinates;
- (3) Offset (expressed in arcsec) of the optical counterpart in the APM catalogue. An upper limit of 5 arcsec indicates those sources missed by our matching procedure, but found in the 2QZ 10k catalogue, as explained in section 2.4;
- (4)  $b_J$  magnitudes; (5)  $(u - b_J)$  and (6)  $(b_J - r)$  colours;
- (7) Radio-flux density (in mJy) at 1.4;
- (8) Redshift;
- (9) Notes on the radio morphological appearance, where  $s$  stands for point-like source,  $d$  for double source (i.e. presenting the two characteristic lobes) and  $t$  indicates a core+lobes structure. This information has been obtained by visual inspection of the images of each source from the FIRST atlas;
- (10) The radio spectral index  $\alpha_R$ , whenever available (see

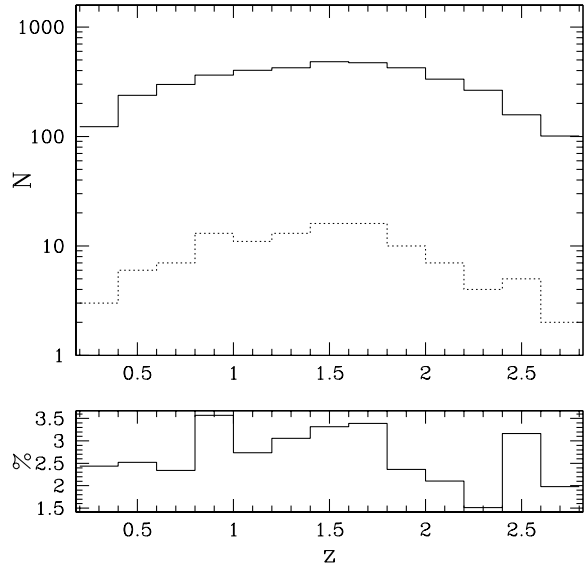


**Figure 3.** Top panel: redshift distribution for the sample of FIRST-2dF QSOs (dotted line) and for all the quasars from the 2QZ 10k catalogue found in the North Galactic Cap (solid line). Bottom panel: ratio between the two distributions.

later in this section).

The redshift distribution of these sources is shown in the top panel of Figure 3 as a dotted line. For comparison, Figure 3 also shows the redshift distribution of the  $\sim 4,000$  quasars from the 2QZ 10k catalogue found in the North Galactic Cap (indicated by the solid line). Interestingly, the two distributions present the same trend, as they both smoothly rise for  $z \gtrsim 0.3$ , exhibit a maximum at about  $z \sim 1.5$  and then decline at higher redshifts. This could be suggestive of a similar fuelling mechanism which controls the birth and life-time of quasars, regardless of their radio-emission.

Note that the observed trend for the two redshift distributions beyond  $z \geq 2.1$  is biased by lack of completeness in the 2QZ 10k sample due to colour selection effects. For this reason, in the following analysis we will only consider objects in the redshift range  $0.35 \leq z \leq 2.1$ . The total number of sources in the FIRST-2dF sample is then reduced to 94, which also includes 3 Broad Absorption Lines QSO (BAL).

The lower panel of Figure 3 shows the ratio between the two redshift distributions. This ratio is found to be  $\sim 3\%$  over the entire redshift range. As it will be extensively discussed in the following sections, the joined effects of selecting sources in the blue band and of using a relatively faint magnitude range, makes the above figure lower than what previously found in literature ( $\sim 10 - 20$  per cent; White et al. 2000; Hewett, Folz & Chaffee 2001; Ivezić et al. 2002).

Figure 4 shows the distribution of  $b_J - r$  colours for the sample of FIRST-2dF quasars (filled squares) as a function of redshift (top panel); a large fraction of sources present values  $0 \lesssim b_J - r \lesssim 1$  (see lower panel), independent of redshift. For comparison, the top panel in Fig. 4 also shows, in small dots, the distribution of  $b_J - r$  colours obtained for

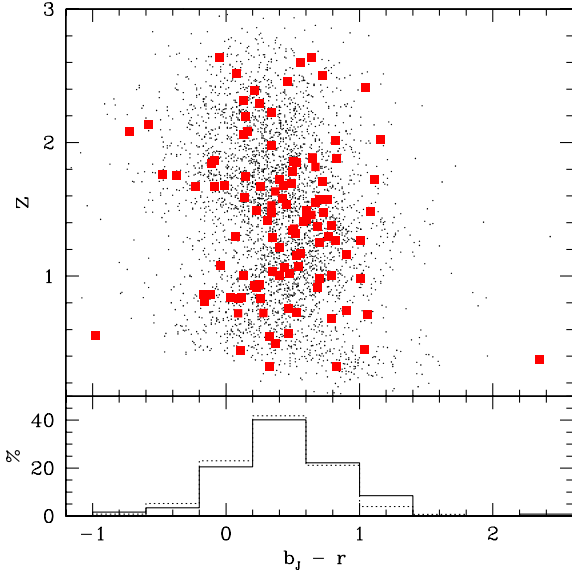


**Figure 4.** Top panel:  $b_J - r$  colours versus redshift for the FIRST-2dF sample (filled squares) as compared with the ones obtained for all the 2QZ 10k quasars in the North Galactic Cap (small dots). The lower panel represents the distributions of  $b_J - r$  colours for the FIRST-2dF sample (solid line) and for all the 2QZ 10k quasars, expressed as a percentage over the total number.

all the 2QZ quasars included in the overlapping FIRST/2dF region (North Galactic Cap). As shown in Figure 5 the distribution of  $b_J - r$  colours is also independent of apparent magnitude and radio flux. It is evident that radio-emitting sources follow the same distribution as the one obtained for the quasar population as a whole, suggestive of a radio activity not related to the colour of the source.

Note that two objects present colours which greatly differ from the average values, the first one showing  $b_J - r > 2$  and the second one having  $b_J - r \lesssim -1$ . This is presumably due to their faint optical magnitudes (found to be  $\sim -21$  and  $\sim -22$  respectively in the first and second case), which allow for a non-negligible light contribution from the host galaxy.

A further piece of information on the nature of sources in the FIRST-2dF sample is given by the investigation of their radio spectral index  $\alpha_R$ \*. In order to measure  $\alpha_R$  we searched for observations performed at different (usually at 5 GHz) wavelengths using NED (NASA/Ipac Extragalactic Database). Unfortunately, as objects in our sample are relatively faint, we only managed to acquire radio fluxes at 5 GHz for the ten most luminous ( $S_{1.4\text{GHz}} \geq 100$  mJy; see Table 1) ones. The distribution of their spectral indices is found to be completely uniform, with five steep spectrum ( $\alpha_R > 0.5$ ) and four flat spectrum ( $\alpha_R < 0.5$ ) sources, plus one object which presents a negative value for the radio spectral index ( $\alpha_R = -0.6$ ).

As the remaining objects do not have any counterpart for radio frequencies  $\nu > 1.4$  GHz, this suggests that sources

\* Throughout this work we define the radio flux density as  $S_\nu \propto \nu^{-\alpha_R}$

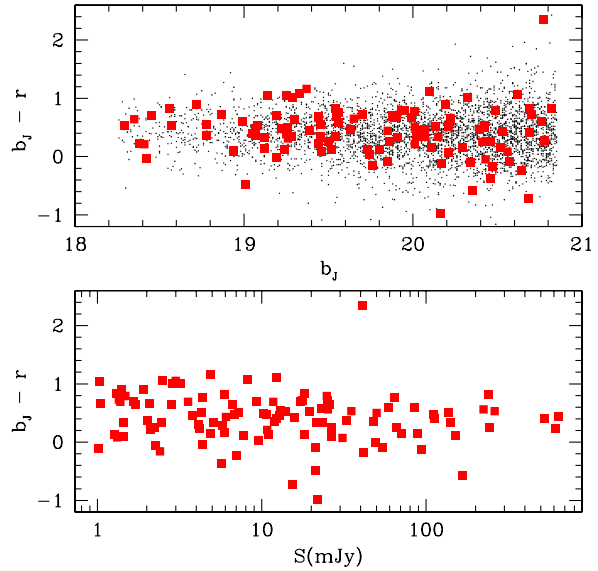


**Figure 5.**  $b_J - r$  colours versus  $b_J$  magnitude (top panel) and radio flux at 1.4 GHz (lower panel). Symbols are as in Figure 4.

in our sample mainly present steep radio spectra, since values  $\alpha < 0.5$  would make at least some of them observable in surveys performed e.g. at 5 GHz. With some confidence we can then assume most of the quasars in the FIRST-2dF sample to have a steep spectrum and associate them to a mean value for the radio spectral index,  $\alpha_R = 0.8$ .

As a final step – in order to facilitate comparisons between our results and those found in literature – we decided to convert magnitudes from the  $b_J$  to the B band. To compute the mean  $B - b_J$  we used the composite quasar spectrum compiled by Brotherton et al. (2001) from  $\sim 600$  radio-selected quasars in the FIRST Bright Quasar Survey (FBQS). It turns out that in the redshift range  $0.3 \leq z \leq 2.2$  the difference between corresponding values in the two bands is very small,  $0.05 \lesssim B - b_J \lesssim 0.09$ , independent of redshift. We therefore chose to apply a mean correction  $B = 0.07 + b_J$ . Note that the k-correction in the B band has also been computed from the Brotherton et al. (2001) composite quasar spectrum.

### 3.2 LBQS

In the previous section we have shown the main observational properties of the FIRST-2dF quasars. Even though  $\sim 100$  radio-emitting QSOs represent one of the widest samples obtained so far, nevertheless – in order to increase the statistics and cover larger portions of the  $M_B - z$  plane – we decided to combine our dataset with other existing samples. Thanks to its selection criteria, the Large Bright Quasar Survey (LBQS) then comes as the natural extension of our original dataset to brighter magnitudes.

A detailed description of this survey can be found in Hewett et al. (1995). Briefly, it consists of quasars optically selected from the APM catalogue (Irwin et al. 1994) at bright ( $b_J < 19$ ) apparent magnitudes. Redshift measurements

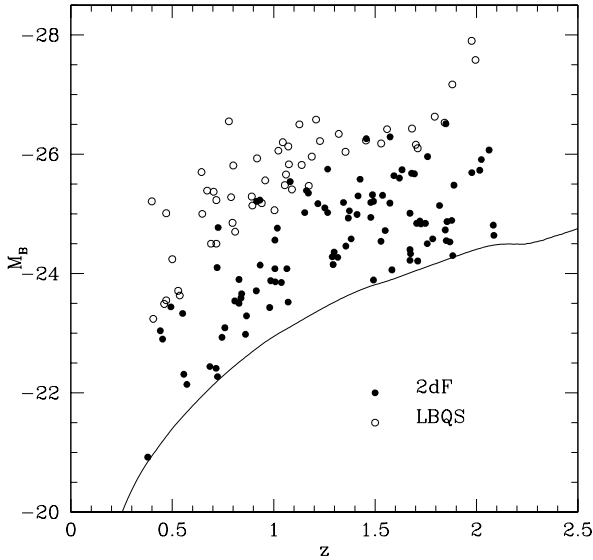


**Figure 6.** Absolute  $M_B$  magnitude versus redshift for the FIRST-2dF (filled circles) and the FIRST-LBQS (empty circles) samples. The solid line describes the selection effect due to the limiting magnitude  $b_J = 20.85$ .

were subsequently derived for 1055 of them over an effective area of 483.8 square degrees. Due to the selection criteria of the survey, quasars were detected over a wide redshift range ( $0.2 \leq z \leq 3.4$ ), with a degree of completeness estimated to be at the  $\sim 90\%$  level.

Recently, this sample has been cross-correlated with the FIRST radio survey (Hewett et al. 2001) by using a searching radius of 2.1 arcsec over an area of 270 square degrees. This procedure yielded a total of 77 quasars (hereafter called the FIRST-LBQS sample) with radio fluxes  $S_{1.4\text{GHz}} \geq 1$  mJy, magnitudes in the range  $16 \lesssim b_J \lesssim 19$ , and fractional incompleteness of  $\sim 10\%$ .

### 3.3 The Combined Sample

The joined FIRST-LBQS and FIRST-2dF samples span an extremely wide range in magnitudes  $-16.5 \lesssim b_J \lesssim 20.85$  – providing a very good coverage of the  $M_B - z$  plane. This can be seen in Figure 6 which represents the distribution of absolute  $M_B$  magnitudes as a function of redshift for the two datasets. In the redshift range where our sample is complete ( $0.35 \leq z \leq 2.1$ ) a wide portion of the  $M_B - z$  plane is filled by sources, and this obtained with the advantage of using only two samples, drawn from the same parent catalogues (FIRST and APM) and with compatible selection criteria.

We remind here that low-redshift, low-luminosity quasars with  $M_B > -23$  have their optical emission dominated by the host galaxy, and will therefore be missed from the 2QZ catalogue as a result of the stellar appearance selection criterion applied to the input catalogue. Following the works by Boyle et al. (2000) and Croom et al. (2001), we then exclude from the dataset all the low-luminosity quasars with  $M_B > -23$ . As Figure 5 shows, this final sample exhibits a full coverage of the  $M_B - z$  plane, except for the

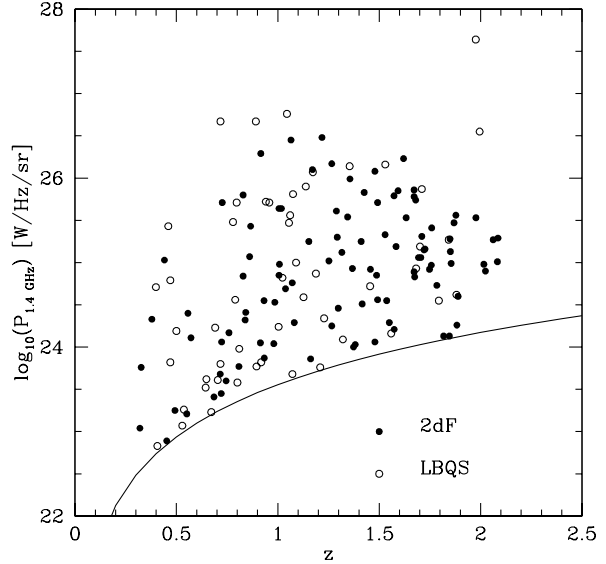


**Figure 7.** Radio-power  $P_{1.4\text{GHz}}$  versus redshift for the FIRST-2dF (filled circles) and the FIRST-LBQS (empty circles) samples. The solid line describes the selection effect due to the limiting flux density of 1 mJy.

narrow region  $-23 \lesssim M_B \lesssim -24$  at  $z \gtrsim 1$ .

Note that the radio power-redshift plane (see Figure 7) is also widely covered; only the region between  $23 \lesssim \log_{10} P_{1.4\text{GHz}} (\text{W Hz}^{-1} \text{sr}^{-1}) \lesssim 24$  is not entirely filled, due to the 1 mJy flux limit of the FIRST survey.

To summarize, our final sample is made of 141 quasars, either coming from the 2QZ 10k catalogue or from the LBQS dataset. These sources, brighter than  $b_J = 20.85$  and  $M_B = -23$ , are found in the redshift range  $0.35 \leq z \leq 2.1$ , and are endowed with a radio counterpart in the FIRST catalogue with  $S_{1.4\text{GHz}} \geq 1$  mJy. The sample is estimated to be  $\gtrsim 90\%$  complete with respect to the optical selection criteria and spectroscopic data acquisition, and 80% complete in its radio component (with a completeness level reaching 100% for fluxes brighter than 3 mJy; see Becker et al. 1995).

In the following sections we will then exploit the potentialities of this sample, homogeneous and deep both in radio and in optical, to investigate the properties of radio-active quasars.

## 4 FRACTION OF RADIO DETECTED QUASARS

A key point on the properties of quasars is the determination of the fraction of radio-emitting sources at a certain flux level, and its possible dependence on redshift and optical luminosity.

As it was shown in Figure 3, from the FIRST-2dF sample we find this fraction to be relatively small ( $\sim 3\%$ ) when compared to previous works ( $\sim 10 - 20$  per cent; White et al. 2000; Hewett, Folz & Chaffee 2001; Ivezić et al. 2002), and independent of redshift. The dependence of the fraction of radio-detected quasars on apparent B magnitude is instead presented in Figure 8, both for the FIRST-LBQS and the

FIRST-2dF samples. Note that with “radio-detected” we indicate all the quasars having radio fluxes greater than 1 mJy and therefore observed by FIRST.

As already noticed by Hewett et al. (2001), we find a significant decrement for increasing magnitudes, with the fraction of radio-detections going from  $\sim 20\%$  at  $B=17$  to  $\sim 2\%$  at  $B=21$ . These values are very different from the 25% of objects with magnitudes  $E \leq 17.8$  deduced by White et al. (2000) from the First Bright Quasar Survey (FBQS). However, Hewett et al. (2001) point out that by applying corrections for the bandpass differences between the LBQS and the FBQS surveys (selected in  $B_J$  and E band respectively), the predicted fraction of radio-detected quasars with magnitudes  $E \leq 17.8$  is found to be 15-17%, which is close to the value obtained for the LBQS sample.

The observed behaviour of the fraction of radio-detected quasars could be explained as either due to an intrinsic dependence of this fraction on optical luminosity, as already suggested by Miller et al. (1990), or as simply given by selection effects. In order to test these hypotheses, in Figure 9 we have plotted the fraction of quasars from both the 2QZ 10k sample and the LBQS that have a counterpart in the FIRST catalogue as a function of the absolute magnitude  $M_B$ , and for the two different redshift bins  $0.35 \leq z \leq 1.3$  and  $1.3 < z \leq 2.1$ .

To minimize the selection effects, we have chosen to use only objects with radio powers  $\log_{10} P_{1.4\text{ GHz}} \geq 24$  ( $\text{W Hz}^{-1}\text{sr}^{-1}$ ), since from Figure 7 it can be seen that the range  $23 \leq \log_{10} P_{1.4}(\text{W Hz}^{-1}\text{sr}^{-1}) < 24$  is not entirely filled with sources due to the 1 mJy flux threshold of the FIRST.

It turns out that the fraction of radio-detected quasars is indeed dependent on their optical luminosity: it grows from  $\lesssim 5\%$  in the case of faint ( $M_B \sim -24$ ) objects, up to  $\sim 20\%$  for the most powerful sources with  $M_B \lesssim -27$ . This trend is present in both of the redshift bins, implying an optical luminosity function for the radio-detected quasars flatter than the one measured for the quasar population as a whole.

This result is in agreement with what found by Goldschmidt et al. (1999) from the Edinburgh Survey, who also observe the fraction of radio-detected QSOs to slightly decrease for increasing look-back times. Our data show something similar but, because of the large error-bars associated to high optical luminosities, this finding does not have great statistical significance.

In fact, if we perform a Kolmogorov-Smirnov (KS) test we find that, while the hypothesis for the two samples of optical quasars and radio-detected ones to have the same distribution in absolute magnitude is discarded at a very high significance level (probability  $\sim 10^{-8}$ ), the same test gives a probability of  $\sim 0.7$  for the data sets to be drawn from the same redshift distribution.

## 5 RADIO LOUDNESS

In this section we will tackle in more detail the issue of radio loudness, with particular attention devoted to the problem of RL/RQ dichotomy.

Two parameters have been proposed to define the radio-loudness of a quasar: the first one is the radio-to-optical

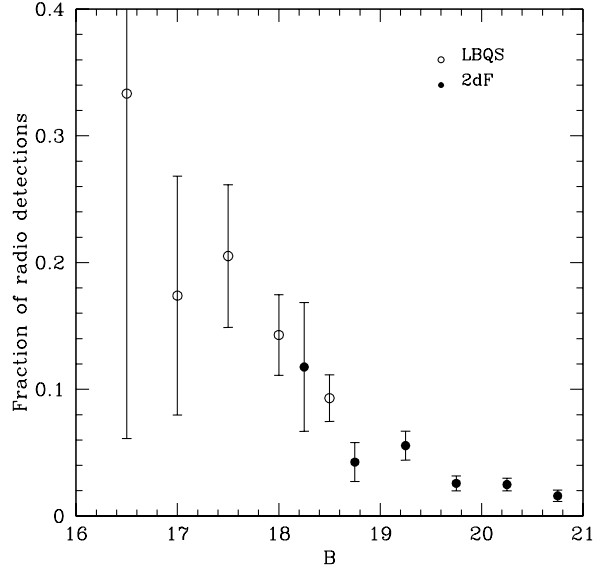


**Figure 8.** Fraction of sources with a counterpart in the FIRST Survey ( $S_{1.4\text{ GHz}} \geq 1$  mJy) for the Large Bright Quasar Survey (empty circles) and 2QZ 10k (filled dots) sample as a function of apparent magnitude.

ratio  $R_\nu^*$  defined as the ratio between the rest frame radio luminosity at a given frequency  $\nu$  and the optical luminosity usually in the B band (Kellermann et al. 1989). Miller et al. (1990) however argued that  $R_\nu^*$  has a physical meaning only if radio and optical luminosities are linearly correlated, and therefore choose the radio power  $P_\nu$  as a better parameter to describe the level of radio loudness.

Several studies which used radio surveys at 5 and 8.5 GHz (Stocke et al. 1992; Padovani 1993; Hooper et al. 1995; Goldschmidt et al. 1999) argued for a gap in the distribution of radio powers and/or radio-to-optical ratios for the objects under exam. The same behaviour was also recently claimed by Ivezić et al. (2002). The presence of a bimodal distribution has been interpreted in the past as direct evidence for quasars to be divided into the two distinct populations of “radio-loud” and “radio-quiet”, with different properties and probably also different mechanisms responsible for the radio emission. The threshold values at which the radio-quiet/radio-loud transition would happen have been inferred by these early works to be  $R_{8.5\text{ GHz}}^* \sim 10$  (corresponding to  $R_{1.4\text{ GHz}}^* \sim 30 - 40$  for objects with spectral index  $\alpha_R = 0.8$ ) or  $\log_{10} P_{5\text{ GHz}} \sim 24$  ( $\text{W Hz}^{-1}\text{sr}^{-1}$ ).

It is worth remarking here that the above definitions are not equivalent. In fact, if we consider our combined FIRST-2dF and FIRST-LBQS dataset and plot the radio-to-optical ratio  $R_{1.4\text{ GHz}}^*$  as a function of radio luminosity  $P_{1.4\text{ GHz}}$  (top panel of Figure 10), it becomes clear that not all the sources (although still a great portion of them) satisfying one of the two criteria can be accepted as radio-loud by the other one. This is the reason why in the following sections – in order to assess the possible presence of a RL/RQ dichotomy in our sample – we will consider both the  $R_{1.4\text{ GHz}}^*$  and  $P_{1.4\text{ GHz}}$  distributions.

Note that if we apply the above definitions for radio loudness

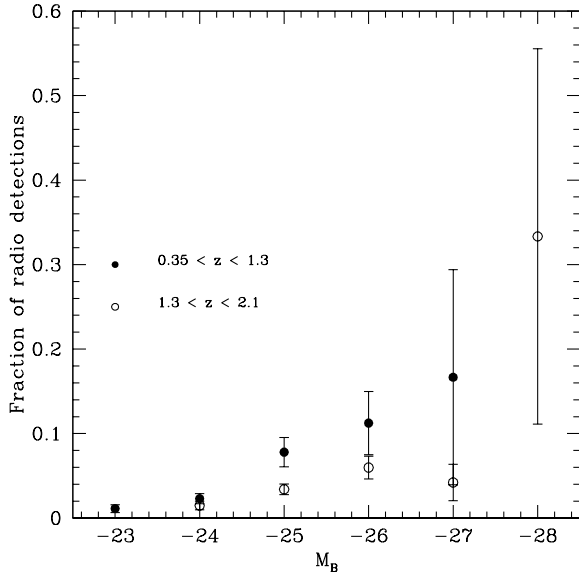


**Figure 9.** Fraction of sources with a counterpart in the FIRST Survey ( $S_{1.4\text{GHz}} \geq 1$  mJy) from both the Large Bright Quasar Survey and 2dF QSO sample as a function of absolute magnitude  $M_B$  in the two redshift ranges:  $0.35 \leq z \leq 1.3$  (filled circles) and  $1.3 < z \leq 2.1$  (empty circles). Only sources with  $\log_{10} P_{1.4} \geq 24$  ( $\text{W Hz}^{-1} \text{sr}^{-1}$ ) have been used in this case.

to the combined sample, we then find  $\sim 75\%$  of the sources to be considered as “radio-loud”, with the remaining  $\sim 30 - 40$  objects probing part of the “radio quiet” regime.

As a last consideration before investigating in more detail the issue of dichotomy, we note that the distribution of radio-to-optical ratios for the combined sample is totally independent of both optical luminosity (middle panel of Figure 10) and redshift (bottom panel of Figure 10). This last finding is in agreement with the results obtained by White et al. (2000) for the First Bright Quasar Survey and Hewett et al. (2001) for the Large Bright Quasar Survey.

### 5.1 No Evidence for a Bimodal Distribution

The previous definitions of radio loudness were introduced in literature because the distributions of radio power and  $R^*$  for the objects under exam appeared to be bimodal. In order to test the presence of this bimodal behaviour in our dataset, we have then considered the distribution of radio-to-optical ratios  $R_{1.4\text{GHz}}^*$  for objects in the combined sample. As Figure 11 illustrates, our data (shown by the solid line) do not present any gap around  $R_{1.4\text{GHz}}^* \sim 40$ , and the distribution appears to be quite flat over a large range of radio-to-optical ratios, the decline observed for  $R_{1.4\text{GHz}}^* \lesssim 30$  being fully consistent with effect of the 1 mJy flux limit of the FIRST survey.

This effect becomes more clear if one considers Figure 12, where the apparent optical magnitude  $B$  has been plotted as a function of the radio flux at 1.4 GHz both for the FIRST-2dF and the FIRST-LBQS samples. The dotted lines represent the loci of constant radio-to-optical ratio. One can then see that the 1 mJy radio limiting flux determines a loss of  $R_{1.4\text{GHz}}^* \lesssim 30$  sources which becomes progressively more

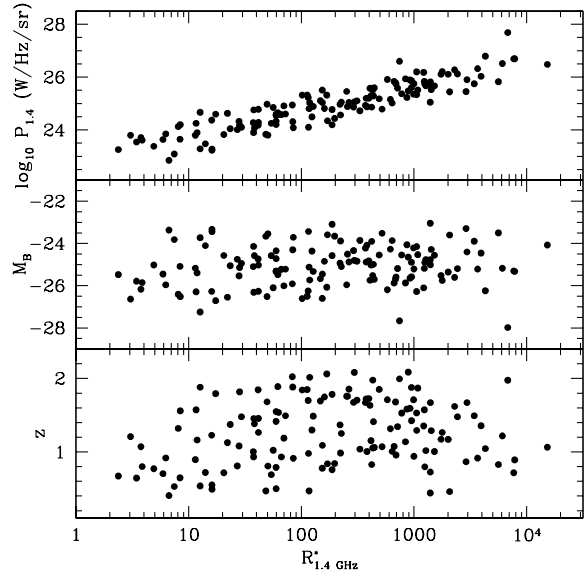


**Figure 10.** Radio-to-optical ratio  $R_{1.4\text{GHz}}^*$  versus radio power (top panel), absolute magnitude (middle panel) and redshift (bottom panel) for the sources in our combined (FIRST-2dF and FIRST-LBQS) sample.

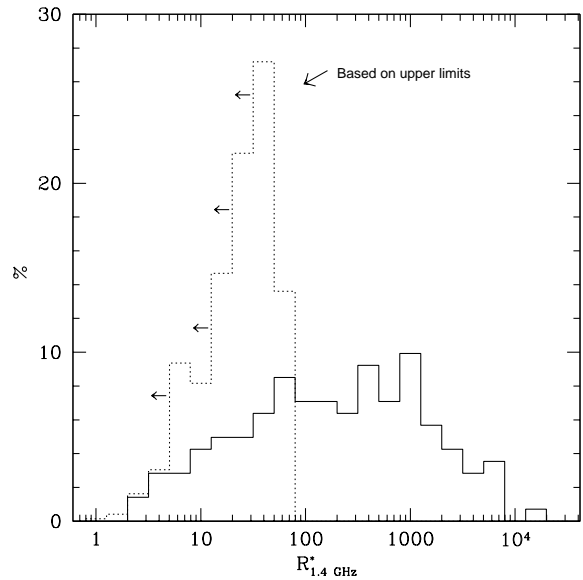


**Figure 11.** Distribution of radio-to-optical ratios  $R_{1.4\text{GHz}}^*$  for the sources in the combined sample expressed in percentages (solid line). The dotted histogram has been obtained for all the quasars found in the North Galactic Cap of the 2QZ 10k catalogue and the Large Bright Quasar Sample which do not have a radio counterpart in the FIRST survey, by assuming an upper flux limit of 1 mJy (see text for details).



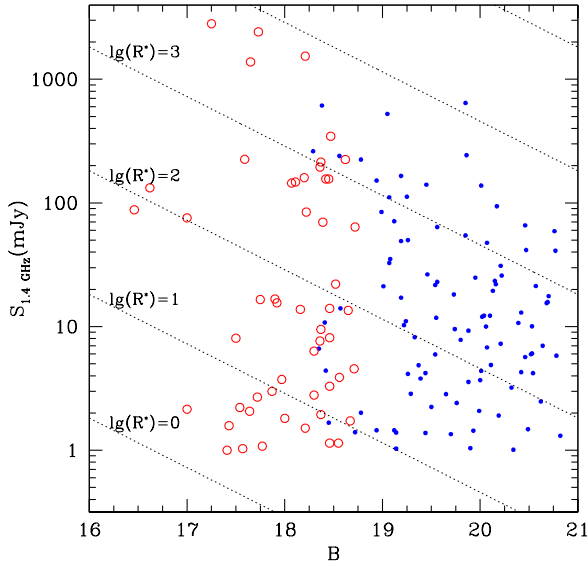


**Figure 12.** Radio flux  $S$  versus  $B$  magnitude for the FIRST-2dF (filled dots) and FIRST-LBQS (empty circles) samples. The dotted lines are the loci of constant radio-to-optical ratio  $R_{1.4\text{ GHz}}^*$  (see text for details).

relevant as the value of the radio-to-optical ratio associated to such objects decreases.

To have an idea of the  $R^*$  distribution of these “missing” sources, we can plot (as shown by the dotted line in Figure 11) the distribution of radio-to-optical ratios for those quasars found in the North Galactic Cap of the 2QZ 10k Survey and in the Large Bright Quasar Survey which do not have a counterpart in the FIRST catalogue, where values for  $R^*$  have been calculated by assuming an upper flux limit of 1 mJy. We can reasonably conclude that our data show no evidence for a  $R_{1.4\text{ GHz}}^* \sim 30 - 40$  gap, in agreement e.g. with the White et al.(2000) results on the FBQS sample.

The presence of a bimodal distribution in the population of quasars has been recently re-claimed by Ivezić et al.(2002) who analysed a sample of radio sources coming from the joined use of the FIRST and Sloan Surveys. We believe their results to be highly biased by the cut both in flux and in magnitude, which preferentially excludes sources with low values of the radio-to-optical ratio and therefore generates an artificial gap in the distribution of  $R^*$  for  $\log_{10} R_{1.4\text{ GHz}}^* \lesssim 2.5$ . In fact, the authors select objects in a region of the apparent magnitude-radio flux plane enclosed by lines perpendicular to the loci of constant radio-to-optical ratios (see their Figure 14). However, we argue that in order to obtain an unbiased  $R_{1.4}^*$  distribution, a weight should be applied to take into account optical number counts, since their steep rise for increasing magnitudes determines a spurious detection of both the apparent peak at large values of  $R_{1.4}^*$  and a lack of sources with low radio-to-optical ratios.

No evidence for a “gap” is seen even if we use the radio-power  $P_{1.4\text{ GHz}}$  as the parameter which separates quasars into radio-quiet and radio-loud ones. We remind here that the assumption for a bimodal distribution as expressed above

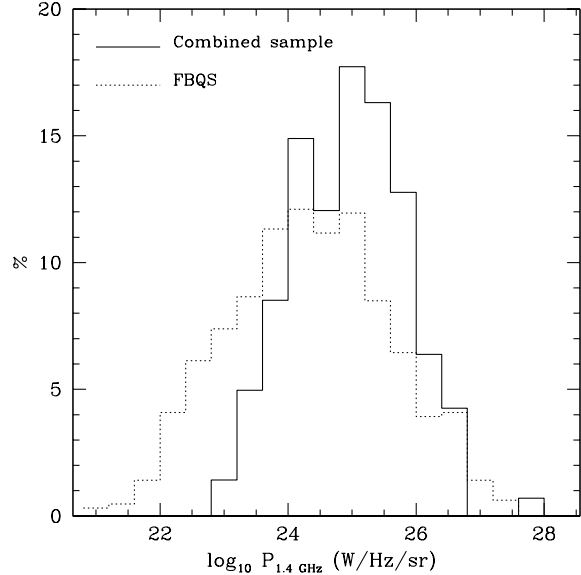


**Figure 13.** Distribution of radio powers for sources of the combined FIRST-2dF and FIRST-LBQS sample (solid line) and in the case of objects from the FBQS (dotted line).

would in fact imply a deficit of sources at radio luminosities  $\log_{10} P_{1.4\text{ GHz}} \sim 24.5$  ( $\text{W Hz}^{-1}\text{sr}^{-1}$ ) (assuming a spectral index  $\alpha_R = 0.8$ ). The absence of a  $P_{1.4\text{ GHz}} \sim 24.5$  gap is clearly shown in Figure 13. Again, the decline observed for  $\log_{10} P_{1.4} \lesssim 24$  ( $\text{W Hz}^{-1}\text{sr}^{-1}$ ) is due to the lack of low-power sources in our sample caused by the 1 mJy completeness limit of the FIRST survey (see Fig. 7). Note that a very similar trend is obtained for quasars from the FBQS (dotted line in Figure 13). Because of the broader redshift range spanned by this survey (different selection criteria allow to also detect low- $z \leq 0.35$  - redshift quasars), the FBQS can provide a better coverage of the faint end of the radio power distribution, even though the 1 mJy limit once again determines the decline of the distribution at low- $\log_{10} P_{1.4\text{ GHz}} \leq 23.5$  ( $\text{W Hz}^{-1}\text{sr}^{-1}$ ) - radio powers. It is nevertheless clear that none of the two distributions hints to the presence of a gap for  $\log_{10} P_{1.4\text{ GHz}} \sim 24.5$  ( $\text{W Hz}^{-1}\text{sr}^{-1}$ ), i.e. to a bimodal distribution for the quasar population.

An alternative way to look at this result is to consider the distribution of radio powers for the objects in our sample as a function of their optical luminosities. As Figure 14 shows, the coverage of the  $L_{\text{radio}} - L_{\text{optical}}$  plane is homogeneous, and the transition from those objects defined as “radio-loud” to those belonging to the “radio-quiet” population extremely smooth. Again, no gap is present, implying a continuous variation in the radio properties of quasars. This is in agreement with e.g. what found by Lacy et al. (2001) from the analysis of sources in the FBQS.

As a final remark, we note (see Figure 14) that there is no tight relationship between radio power and optical luminosity for the objects in our combined sample, since sources with a particular luminosity  $L_{\text{optical}}$  can be endowed with radio powers spanning up to three orders of magnitude. From the above result we can also have some hints that the ra-

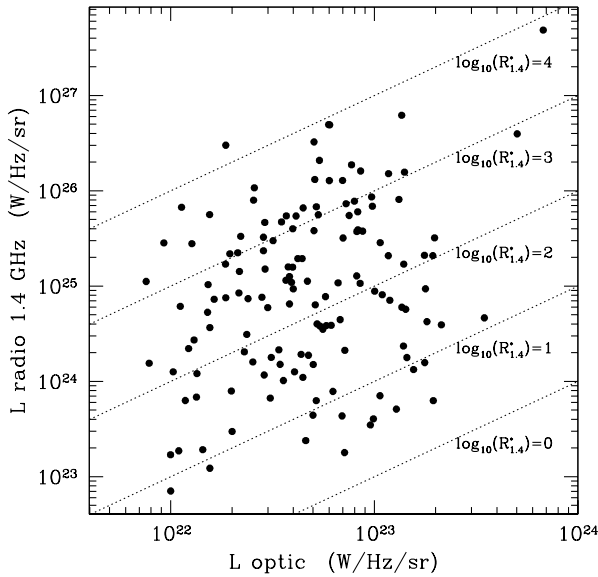


**Figure 14.** Optical luminosity versus radio power for sources in the combined FIRST-2dF and FIRST-LBQS sample. The dotted lines are the loci of constant radio-to-optical ratio.

radio properties of quasars are not related to the mass of the central black hole. In fact, in the case of quasars it has been shown that the optical emission is tightly related to the bolometric one (Elvis et al. 1994). We can reasonably assume that these bright quasars are emitting close to the Eddington limit and in this case the bolometric luminosity can in turn be connected to the mass of the central black hole. Since we find a very spread relation between radio and optical luminosity, it seems unlikely that the mass of the central black hole dominates the level of radio emission.

## 6 CONCLUSIONS

We have presented a new sample of radio-emitting quasars, obtained by matching together objects from the FIRST and 2dF Quasar Redshift Surveys. The dataset includes 113 quasars, found within the redshift range  $0.3 \leq z \leq 2.2$ , with optical magnitudes  $18.25 \leq b_J \leq 20.85$  and radio fluxes at 1.4 GHz  $S \geq 1$  mJy.

This sample has then been combined with the FIRST-LBQS catalogue (Hewett et al. 2001) in order to provide an almost-complete coverage of the optical luminosity-redshift plane and increase the statistical significance of our results. The main conclusions deriving from the joined analysis of the two samples can be summarized as follows:

(i) The properties of radio-emitting quasars, such as their redshift distribution and  $b_J - r$  colours, are in full agreement with those derived for the quasar population as a whole. This suggests the fuelling mechanism(s) responsible for the birth, colour and life-time of quasars to be independent of the level of radio emission.

(ii) The fraction of radio detections decreases for fainter apparent magnitudes. This is also true if one considers the intrinsic luminosity of the sources, as the fraction of radio

detections is found to grow from  $\lesssim 3\%$  at  $M_B \sim -24$  up to 20-30 % for the brightest ( $M_B \sim -28$ ) objects.

(iii) The classical radio loud/radio quiet dichotomy, in which the distribution of radio-to-optical ratios and/or radio luminosities shows a “gap”, has been ruled out by our analysis. We found no lack of sources neither for  $R_{1.4\text{GHz}}^* \sim 30-40$  nor for  $\log_{10} P_{1.4} \sim 24$  ( $\text{W Hz}^{-1}\text{sr}^{-1}$ ). Due to the selection effects – in particular the 1 mJy radio flux limit of the FIRST survey – we could not explore the low-P/low- $R^*$  regions of the distributions. However, at least in the observed ranges, it is suggestive of a smooth transition from the radio-loud to the radio-quiet regime.

(iv) We find no tight relationship between radio and optical luminosity for the sources in our sample. For a given optical luminosity the scatter in the radio power is found to be more than three orders of magnitude. This result can give us some insight on the physical quantities responsible for the radio emission. In fact – since in the case of quasars the optical emission is tightly related to the bolometric one (Elvis et al. 1994), the bolometric luminosity (under the assumption that quasars emit close to the Eddington limit) can in turn be connected to the mass of the central black hole – such a large scatter tends to exclude the mass of the central black hole as the relevant quantity which controls the level of radio activity.

It is clear that the above results – especially those concerning the radio-quiet/radio-loud dichotomy – need further investigation. While awaiting for wide-area surveys able to probe the low radio-power/low radio-to-optical ratio regime, we are testing the nature and behaviour of the radio emission of quasars, through Monte Carlo simulations. We plan to tackle this issue in a future paper.

## ACKNOWLEDGMENTS

We acknowledge the Italian MIUR and ASI for financial support.

## REFERENCES

- Becker R.H., White R.L., Helfand D.J., 1995, *ApJ*, 450, 559  
 Blandford R.D., 2000, *PTRSA*, astro-ph/0001499  
 Boyle B.J., Shanks T., Croom S.M., Smith R.J., Miller L., Loaring N., Heymans C., 2000, *MNRAS*, 317, 1014  
 Brotherton M.S., Tran H.D., Becker R.H., Gregg M.D., Laurent-Muehleisen S.A., White R.L., 2001, *ApJ*, 546, 775  
 Condon J.J., O’Dell S.L., Puschell J.J., & Stein W.A. 1981, *ApJ*, 246, 624  
 Condon J.J., Cotton W.D., Greisen E. W., Yin Q.F., Perley R.A., Taylor G.B., Broderick J.J., 1998, *AJ*, 115, 1693  
 Croom S.M., Smith R.J., Boyle B.J., Shanks T., Loaring N.S., Miller L., Lewis I.J., 2001, *MNRAS*, 322, L29  
 Dunlop J.S., McLure R.J., Kukula M.J., Baum S.A., O’Dea C.P., Hughes D.H., 2002, astro-ph/0108397  
 Ellingson E., Yee H.K.C., Green R.F., 1991, *ApJ*, 371, 49  
 Elvis M., Wilkes B.J., McDowell J.C., Green R.F., Bechtold J., Willner S.P., Oey M.S., Polomski E., Cutri R., 1994, *ApJS*, 95, 1  
 Finn R.A., Impey C.D., Hooper E.J., 2001, *ApJ*, 557, 578  
 Goldschmidt P., Kukula M.J., Miller L., Dunlop J.S., 1999, *ApJ*, 511, 612

- Hewett P.C., Foltz C.B., Craig B., Chaffee F.H., 1995, *AJ*, 109, 1498
- Hewett P.C., Foltz C.B., Chaffee F.H., 2001, *AJ*, 122, 518
- Hooper E.J., Impey C.D., Foltz C.B., Hewett P.C., 1995, *ApJ*, 445, 62
- Irwin M.J., McMahon R.G., Maddox S.J., 1994, *Spectrum*, 2, 14
- Ivezic Z., Menou K., Strauss M., Knapp G.R., Lupton H.R., vanden Berk D.E., Richards G.T.; Tremonti C., Weinstein M.A., Anderson S., et al., 2002, *AJ*, 124, 2364
- Kellermann K.I., Sramek R., Schmidt M., Shaffer D.B., Green R., 1989, *AJ*, 98, 1195
- Lacy M., Laurent-Muehleisen S.A., Ridgway S.E., Becker R.H., White R.L., 2001, *ApJL*, 551, L17
- La Franca F., Gregorini L., Cristiani S., De Ruiter H., Owen F., 1994, *AJ*, 108, 1548
- Maddox S.J., Efstathiou G., Sutherland W.J., Loveday J., 1990, *MNRAS*, 243, 692
- Magliocchetti M., Maddox S.J., Lahav O., Wall J.V., 1998, *MNRAS*, 300, 257
- Magliocchetti M., Maddox S.J., 2002, *MNRAS*, 330, 241
- Magliocchetti M., Maddox S.J., Jackson C.A., Bland-Hawthorn J., Bridges T., et al., 2002, *MNRAS*, 333, 100
- Malkan M.A., 1984, *ApJ*, 287, 555
- Marshall H.L., 1987, *ApJ*, 316, 84
- McMahon R.G., White R.L., Helfand D.J., Becker R.H., 2002, *ApJS*, 143, 1
- Miller L., Peacock J.A., Mead A.R.G., 1990, *MNRAS*, 244, 207
- Padovani P., 1993, *MNRAS*, 263, 461
- Sandage A., 1965, *ApJ*, 141, 1560
- Schmidt M., 1963, *Nature*, 197, 1040
- Smith E.P., Heckman T.M., Bothun G.D., Romanishin W., Balick B., 1986, *ApJ*, 306, 64
- Sramek R.A., & Weedman D.W., 1980, *ApJ*, 238, 435
- Stocke J.T., Morris S.L., Weymann R.J., Foltz C.B., 1992, *ApJ*, 396, 487
- Voges W., Aschenbach B., Boller T., Bräuninger H., Briel U., et al., 1999, *AA*, 349, 389
- White R.L., Becker R.H., Helfand D.J., Gregg M.D., 1997, *ApJ*, 475, 479
- White R.L., Becker R.H., Gregg M.D., Laurent-Muehleisen S.A., Brotherton M.S., et al., 2000, *ApJS*, 126, 133
- Yee H.K.C. & Green R.F., 1987, *ApJ*, 319, 28